ELSEVIER

International Journal of Mass Spectrometry 185/186/187 (1999) 281–289

International Journal of Mass Spectrometry

A Fourier transform ion cyclotron resonance study of two- and one-electron capture reactions between doubly charged rare gas ions and rare gas atoms

Holger von Köding, Nico M. M. Nibbering*

Institute of Mass Spectrometry, University of Amsterdam, Nieuwe Achtergracht 129, 1018 WS Amsterdam, The Netherlands

Received 1 June 1998; accepted 24 August 1998

Abstract

A Fourier transform ion cyclotron resonance (FTICR) mass spectrometer has been used to study near thermal collision energy symmetric charge transfer reactions. The systems Xe^{n+}/Xe, Kr^{n+}/Kr and Ar^{n+}/Ar have been measured at ambient temperature, where $n = 1, 2$. In the interactions between doubly charged rare gas ions and their corresponding neutral gas atoms the double electron capture (DEC) has been observed to be more efficient than the single electron capture (SEC). From the measured overall rate coefficient of 3.4×10^{-10} cm^3 s^{-1} and the branching ratio of 1.1 between the DEC reaction and the SEC reaction the rate coefficients for double and single electron transfer from Xe to Xe^{2+} have been calculated to be 1.8×10^{-10} cm^3 s^{-1} and of 1.6×10^{-10} cm^3 s^{-1}. In the experiments with doubly charged krypton and doubly charged argon ions in their parent gases the symmetric double charge transfer is observed to be even more favored in comparison with the Xe^{2+}/Xe system at near thermal collision energies. (Int J Mass Spectrom 185/186/187 (1999) 281–289) © 1999 Elsevier Science B.V.

Keywords: Fourier transform ion cyclotron resonance; Two-electron capture; Doubly charged rare gas ions, Rate coefficients, Rare gas ion/atom reactions

1. Introduction

The research on collision processes of multiply charged ions with neutral atomic particles has become one of the most challenging topics in atomic collision physics during the last two decades. The understanding of the fundamental collision dynamics makes it possible to explain numerous phenomena found in plasmas which contain multiply charged ions. Their presence has an enormous impact on the main plasma properties because of the strongly enhanced cross section of their collision processes compared with singly charged ions. The gained advance of our basic knowledge has stimulated the search for new radiation sources in laser physics, in particular in the XUV and x-ray region of the electromagnetic frequency spectrum. In gas-phase ion chemistry electron transfer reactions between multiply charged ions and atoms or molecules have been preferably studied previously in the high energy collision domain ($E_{coll} \geq 1$ keV) [1–5]. In the intermediate collision energy range (2 eV $\leq E_{coll} \leq 1$ keV) the symmetric resonance double charge transfer cross section of doubly charged argon

* Corresponding author.

Dedicated to Professor Mike T. Bowers on the occasion of his 60th birthday with thanks for his many basic contributions to mass spectrometry.

PII S1387-3806(98)14155-6

in argon gas has been determined by a merging-beam technique [6]. Only a few papers have been published which describe at very low collision energy conditions ($E_{coll} \leq 2$ eV) single and/or double electron transfer of doubly charged ions in their rare gases as observed in a drift-tube mass spectrometer [7–9]. Other publications report single and double electron transfer from simple atoms and molecules to Ar^{2+}, Mg^{2+}, Ca^{2+}, He^{2+}, Kr^{2+}, Xe^{2+}, Ne^{2+} and Nb^{2+} ions [10–17] and in terms of multi-electron capture processes the interaction between C^{4+} ions and simple aliphatic hydrocarbons [18]. The present study of two- and one-electron capture reactions between doubly charged rare gas ions and rare gas atoms is a more elaborate follow-up of our preliminary reports [19,20] on the Xe^{2+}/Xe system.

2. Experimental

The experiments were performed using a Bruker Apex 47e Fourier transform ion cyclotron resonance (FTICR) mass spectrometer (Bruker Daltonics, Billerica, MA, USA), equipped with a 4.7 T superconducting magnet, an external ion source and a Bruker cylindrical "infinity" cell with a diameter of 6.0 cm [21]. Any experiment is controlled by Bruker's XMASS [22] processing and acquisition software package running under the UNIX [23] operating system which is installed on a Silicon Graphics work station. The general operating procedures for careful ion manipulation (selection/detection) have been described previously [24,25].

One of the most advantageous features of the FTICR-MS method is the "nondestructive" manner of ion detection. However, the intensity of the detected signal strongly depends on the translational excitation process of the ions performed prior to and necessary for detection. In previous publications [26–36] various experimental conditions have been discussed which might affect the relative ion abundances to be measured. In this study the excitation spectrum of the power amplifier and associated circuitry was measured, because one prerequisite for accurate measurements of relative peak intensities is that all ions to be detected are excited to the same ion cyclotron orbit and thus induce the same response signal in the detection plates. Fig. 1 shows the root-mean-square (rms) output voltage, U_{rms}, as a function of the mass-to-charge ratio m/z. Using standard formulae to convert U_{rms} into the resulting exciting rf electric field, E_0, indicates that E_0 increases by a factor of about 1.65 when a frequency range corresponding to $m/z = 20$ i.e. $^{40}Ar^{2+}$ up to $m/z = 132$ i.e. $^{132}Xe^{\cdot+}$ is covered. This measurement indicates the necessity to correct for the nonuniform excitation field in order to obtain and use the correct relative ion abundances when rate coefficients and branching ratios are determined in ion/molecule reactions. Fig. 1 also indicates that a remarkable deviation from uniformity only is observed for frequencies $\nu \geq 0.5$ MHz, that is $m/z \leq 145$, at the magnetic field strength of 4.7 T of the instrument used.

All gases used in this study were commercially available and were used without further purification [methane (quality 99.995%) and argon gas (quality 99.999%), Hoek Loos B.V., Schiedam, The Netherlands; xenon gas (quality 99.995%) and krypton gas (quality 99.990%), Air Liquide B.V., Eindhoven, The Netherlands; argon-36 gas (quality 99.50%), Campro Scientific B.V., Veenendaal, The Netherlands]. In each experiment, methane (used for calibration of the pressure in the FTICR cell, see [20]), argon, krypton and xenon gas were leaked into the cylindrical cell via a needle capillary system. The cell was kept at room temperature. The ions were generated inside the ICR cell by electron ionization (EI) at gas pressures and experimental parameters mentioned in Tables 1 and 2 and in the legends of the figures, respectively. In all experiments the singly and doubly charged rare gas ions have been translationally cooled by collisions with its neutral gas prior to ion selection. This procedure is applicable when the charge transfer reaction is not collision controlled. In all reactions involving singly and doubly charged reactant ions relaxation time periods up to eight seconds were applied. During this period the ions were allowed to relax into their electronic ground states and to reduce their trapping oscillation parallel to the magnetic field. Afterwards, in order to select one specific isotopic

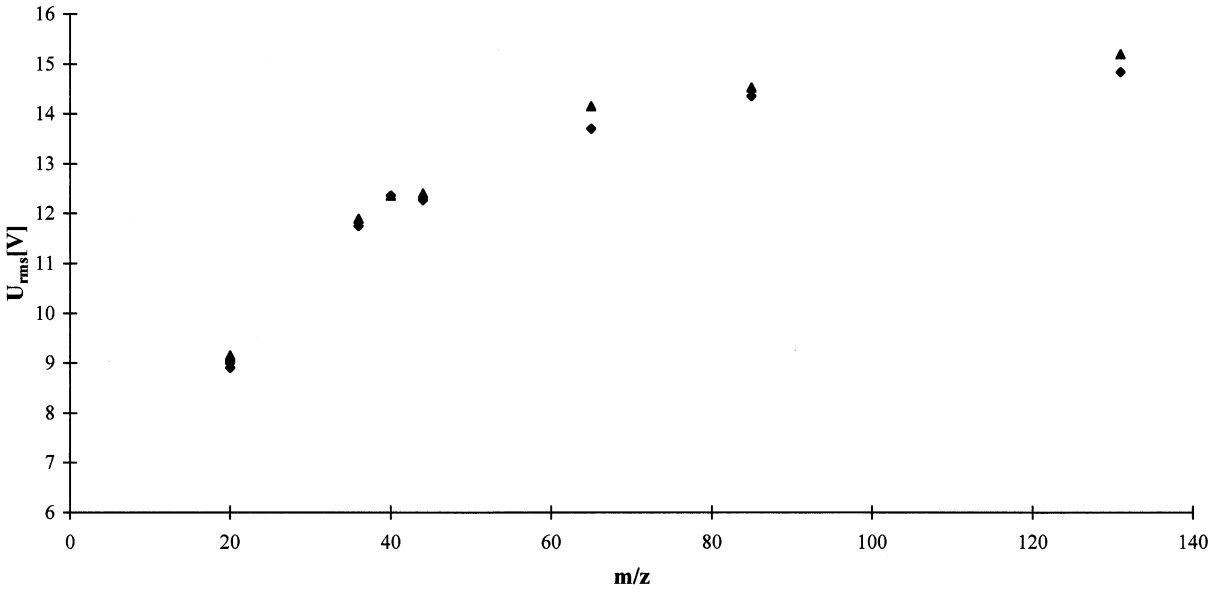

Fig. 1. Measured root-mean-square (rms) output voltage, U_{rms}, of the power amplifier and associated circuitry as a function of the mass-to-charge ratio m/z at 5 dB attenuation level. The voltages have been measured on both excitation plates, as indicated by the two kinds of symbols, to give proof of an entirely symmetric ion excitation process.

reactant ion ensemble all other ions have been brought to ion trajectories exceeding the radial dimension of the cylindrical cell by applying a sequence of single radio frequency shots at frequencies corresponding to the reduced ion cyclotron frequency ω_+ of the mass-to-charge ratio m/z of the unwanted ions. This procedure has been applied in any single experiment and in this way the selection of a specific reactant ion has been performed prior to the study of its reaction kinetics with the neutral rare gas atoms.

In the symmetric charge transfer experiments performed in this study, one possible charge transfer process is observed to happen from the reactant ion to its neutral counterpart (see Scheme 1 below). That

Table 1
Experimental conditions used for studying the single charge transfer reactions between $^{136}Xe^{\cdot+}$, $^{86}Kr^{\cdot+}$, and $^{36}Ar^{\cdot+}$ and their natural rare gas atoms

Reactant ion	$^{136}Xe^{\cdot+}$	$^{86}Kr^{\cdot+}$	$^{36}Ar^{\cdot+}$
Trapping potential [V]	0.76	0.76	0.76
Target pressure [Pa]	6.9×10^{-6}	3.1×10^{-6}	5.4×10^{-6}
E (ionizing electrons) [eV]	35	25	35
t (ionization) [ms]	250	250	250
Buffer gas for ion relaxation	Xe	Kr	Ar
t (relaxation) [s]	4	3	8
t (ejection shots) [ms]	2.3	2.3	2.3
Electric field E_0 [V/m]	400	272	315
r (ejection) [cm]	4.9	3.3	4.7
Reaction time [s]	0–0.9	0–1.2	0–1.0

Table 2
Experimental conditions used for studying the double charge transfer reactions between $^{136}Xe^{2+}$, $^{86}Kr^{2+}$ and $^{40}Ar^{2+}$ and their natural rare gas atoms

Reactant ion	$^{136}Xe^{2+}$	$^{86}Kr^{2+}$	$^{40}Ar^{2+}$
Trapping potential [V]	2.28	2.28	2.28
Target pressure [Pa]	6.3×10^{-6}	3.5×10^{-6}	4.5×10^{-6}
E (ionizing electrons) [eV]	100	100	100
t (ionization) [ms]	500	500	500
Buffer gas for ion relaxation	Xe	Kr	Ar
t (relaxation) [s]	4	4	4
t (ejection shots) [ms]	2.3	2.3	2.3
Electric field E_0 [V/m]	370	265	271
r (ejection) [cm]	4.5	3.2	3.3
Reaction time [s]	0–0.6	0–0.6	0–0.7

means, that after a given reaction delay the total ion peak intensity at this specific mass-to-charge ratio is the sum of the peak intensities corresponding to the remaining reactant ion abundance and the formed product ion abundance of the same mass-to-charge ratio. Assuming, that the relative product ion abundances are only determined by the isotopic distribution of the target gas, which isotopic distribution is known, one can distinguish between the decaying reactant ion abundance and the arising product ion abundance. Therefore the natural abundances of xenon and krypton gas have been used to calculate the remaining percentage of the reactant ion by subtracting the product ion peak intensity from the total intensity of the reactant ion isotope peak. The slope resulting from the logarithmic plot of the decaying abundance of the reactant ion as a function of time has been used to calculate the rate coefficients. In the study of the charge transfer reaction between singly or doubly charged argon ions in its parent gas the natural argon gas isotopic composition has been modified. The natural abundances of the three stable argon isotopes are ^{40}Ar: ^{38}Ar: ^{36}Ar = 99.6: 0.063: 0.337. Accurate quantitative measurements of relative peak heights based on such very large differences in abundance are hardly accessible by use of the ICR technique. Therefore, in order to measure the charge transfer rate coefficient, the natural argon gas has been enriched by isotopic pure ^{36}Ar gas. The composition of the enriched gas mixture appeared to be ^{40}Ar: ^{36}Ar = 100: 29.5 and has been determined after electron ionization ($t_{\text{ionization}}$ = 5 ms, E_{e} = 30 eV, V_{trap} = 0.76 V) prior to detection in the broadband detection mode. This gas mixture has been used to study the single electron transfer to singly charged $^{36}Ar^{\cdot+}$ ions. The same procedure of sample preparation has been applied to the argon gas sample which was used to study the electron transfer to the doubly charged reactant ion $^{40}Ar^{2+}$. In this experiment the sample composition has been determined to be ^{40}Ar: ^{36}Ar = 100: 52.5. Using these relative abundances the decay of the Ar^{n+} reactant ion was followed as above described for the xenon and krypton experiments.

3. Results and discussion

Fig. 2 shows the spectrum of isolated $^{86}Kr^{\cdot+}$ recorded in the broadband detection mode and in a second spectrum the progress of the reaction between the isolated $^{86}Kr^{\cdot+}$ ions and neutral krypton gas after a reaction time of 0.6 s. The krypton product ions appear in their natural abundance. This illustrates the good performance of the FTICR method with regard to measuring relative ion abundances.

Using the above mentioned experimental parameters it has been possible to trap singly charged krypton ions with an efficiency of at least 95% at any time during the reaction. The logarithmic decay of the ion abundance of the reactant $^{86}Kr^{\cdot+}$ ions as a function of time is plotted in Fig. 3.

Fig. 4 displays the spectrum of isolated $^{86}Kr^{2+}$ ions and the corresponding spectrum obtained after a reaction time of 0.5 s. From Fig. 4 it can be seen that peaks because of singly and doubly charged krypton isotopes are present.

In this experiment the trapping plates were held on 2.28 V. Assuming that the kinetic energy, that an ion may gain, arises essentially from the electrostatic potential at the position of ion generation, the kinetic energy distribution of the doubly charged reactant ions would range from near thermal energies up to ~2 eV immediately following the ion generating event. The kinetic energy distribution of the target gas atoms can be approximated by the Poisson distribution. Using the kinetic gas theory together with this approximation the probabilities for single or multiple collisions during a given period of time, that is the relaxation period of 4 s long and the reaction time window, which never exceeds 0.6 s, can be calculated, respectively [37,38]. The calculation indicates that Kr^{2+} ions undergo approximately four collisions with the target gas atoms within the relaxation period. The probability, that during the reaction time period of 0.6 s a second collision occurs is computed to be 0.07 for an estimated center-of-mass collision energy of 0.125 eV, which indicates essentially single collision conditions. Thus, the krypton target pressure and the translationally cooling of the $^{86}Kr^{2+}$ ions ensures that the reaction progresses under single collision condi-

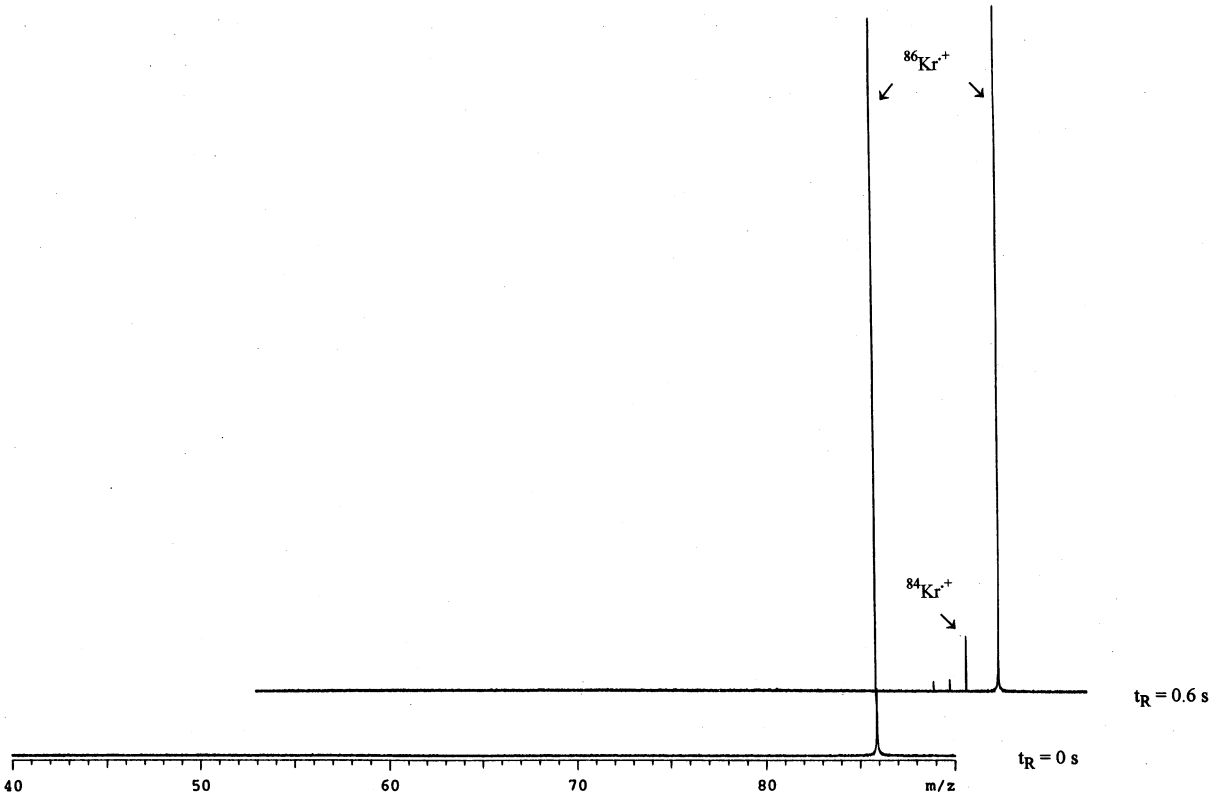

Fig. 2. Spectra showing the selection of $^{86}Kr^{\cdot+}$ ions and after ejection of all other ions from the FTICR cell at a neutral krypton gas pressure of 3.1×10^{-6} Pa (bottom) and the progress of the reaction with neutral krypton gas after a reaction time t_R of 0.6 s (top). The energy of the ionizing electrons was set at 25 eV to generate singly charged krypton. Prior to Fourier transformation 300 signals were accumulated. The response signal was sampled for 26.2 ms. For other conditions, see Table 1.

tions. Therefore not only single electron capture (SEC) also double electron capture (DEC) is observed within a single reactant ion/neutral target collision. Experiments utilizing trapping voltages up to 3.5 volts have also been performed without observing a change in the ratio between singly and doubly charged product ions. In any experiment the ion trapping efficiency has been observed to be more than 90%. After correcting the observed ion abundances for the excitation spectrum provided by the frequency synthesizer (see Experimental) the overall rate coefficient has been determined to be 4.8×10^{-10} cm^3 s^{-1}. Moreover, from the sums of singly and doubly charged product ions a branching ratio of 2.9 between double and single electron transfer from Kr to Kr^{2+} has been calculated. This would indicate that the rate coefficient for double and single electron transfer would be 3.5×10^{-10} cm^3 s^{-1} and 1.2×10^{-10} cm^3 s^{-1}, respectively. In the same way the rate coefficients for the $^{136}Xe^{2+}$/Xe and $^{40}Ar^{2+}$/Ar systems have been obtained and summarized in Table 3. All rate coefficients listed in Table 3 (see seventh and twelfth to fourteenth row) have an estimated error of $\pm$20%, that mainly originates from the uncertainty of the real ICR cell pressure determination. For comparison, the results of other groups as far as available have been included in Table 3.

Previous studies using the selected ion flow tube (SIFT) [10] and a drift-tube mass spectrometer [39], respectively, have confirmed that electron capture processes not only depend on the charge state, but also on the electronic state of the projectile resulting

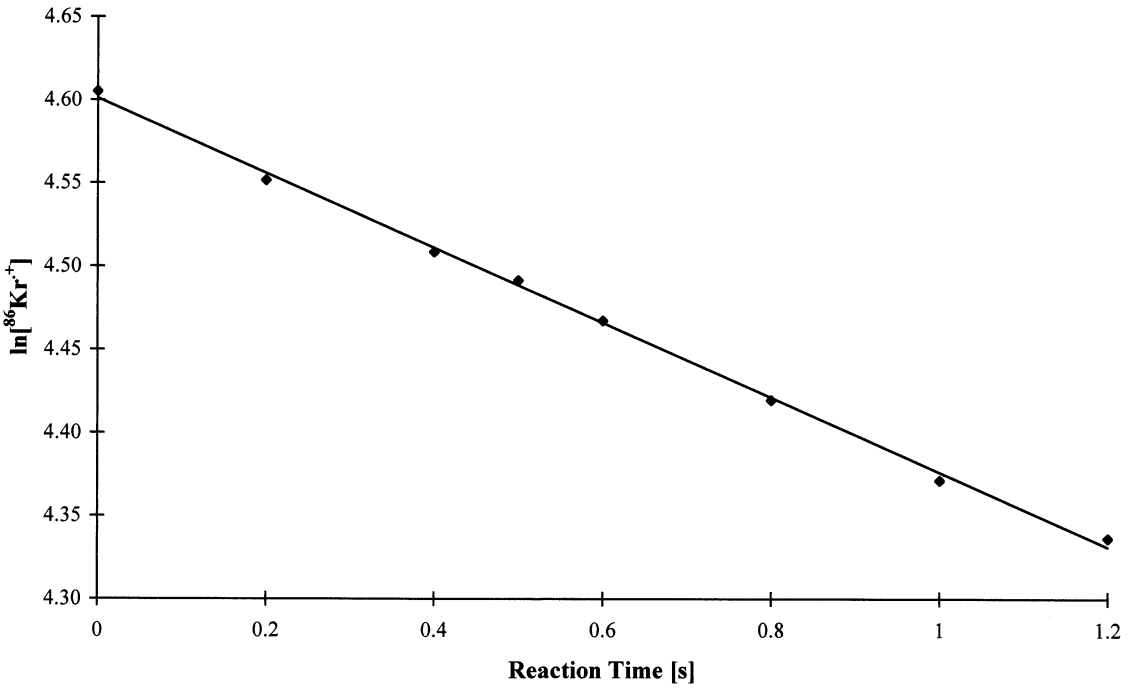

Fig. 3. Logarithmic decay of the reactant ion $^{86}Kr^{\cdot+}$ abundance. The corresponding peak intensities were measured by recording of spectra in the broadband detection mode. For other conditions see Table 1.

in state selective rate coefficients in ion/molecule reactions that can vary by orders of magnitude. The authors of these studies also observed the state selective symmetric single electron transfer from rare gas atoms to doubly charged rare gas ions to occur at very low rate coefficients (usually between 10^{-12} and 10^{-14} cm^3 s^{-1}). In particular they concluded from their measurements that (^{3}P)Ar^{2+} did not significantly react with argon gas atoms while (^{1}S$_0$)Ar^{2+} did react at a rate of 6×10^{-12} cm^3 s^{-1}. Taking the measured lifetime of (^{1}S$_0$)Ar^{2+} [41] to be τ = 159.7 ms (see Table 3) then after our relaxation period of 4 s no significant (^{1}S$_0$)Ar^{2+} ion abundance should be present in the ICR cell before measuring of the reaction kinetics is started for the reaction between an initial (^{3}P)Ar^{2+} projectile ion with atomic argon gas. Their estimated rate coefficient of about 10^{-14} cm^3 s^{-1} for the single electron capture in this system [10,39] turns out to be about four orders of magnitude lower than we have measured (see Table 3). In a more recent study Prior [43] has investigated the Ar^{2+}/Ar system using an electrostatic trap of the type first used by Kingdon [44]. Prior obtained a considerably higher rate coefficient ($k = 5.5 \times 10^{-10}$ cm^3 s^{-1}) for the (^{1}S$_0$)Ar^{2+}/Ar system. Furthermore, the overall reaction rate coefficient was reported to be $k = 8.9 \times 10^{-10}$ cm^3 s^{-1} within the studied reaction window, which was up to 80 ms long [43]. From the statistical electronic state distribution of Ar^{2+} ions it was concluded that the total ion decay should be dominated by the metastable (^{1}D$_2$)Ar^{2+} state and the (^{3}P)Ar^{2+} ground state and in that way the discrepancy between both measured rate coefficients was explained [43]. Okuno [45] published in 1986 single and double electron-capture cross sections of Ar^{2+} and Kr^{2+} ions in their parent gases. In that study a beam guide technique was applied covering a collision energy range from 0.40–500 eV (Ar^{2+}/Ar system) and 0.25–804 eV (Kr^{2+}/Kr system). The cross section for the double electron transfer process σ_{20} was calculated from measurements of the ion intensities corresponding to the incident doubly charged ion

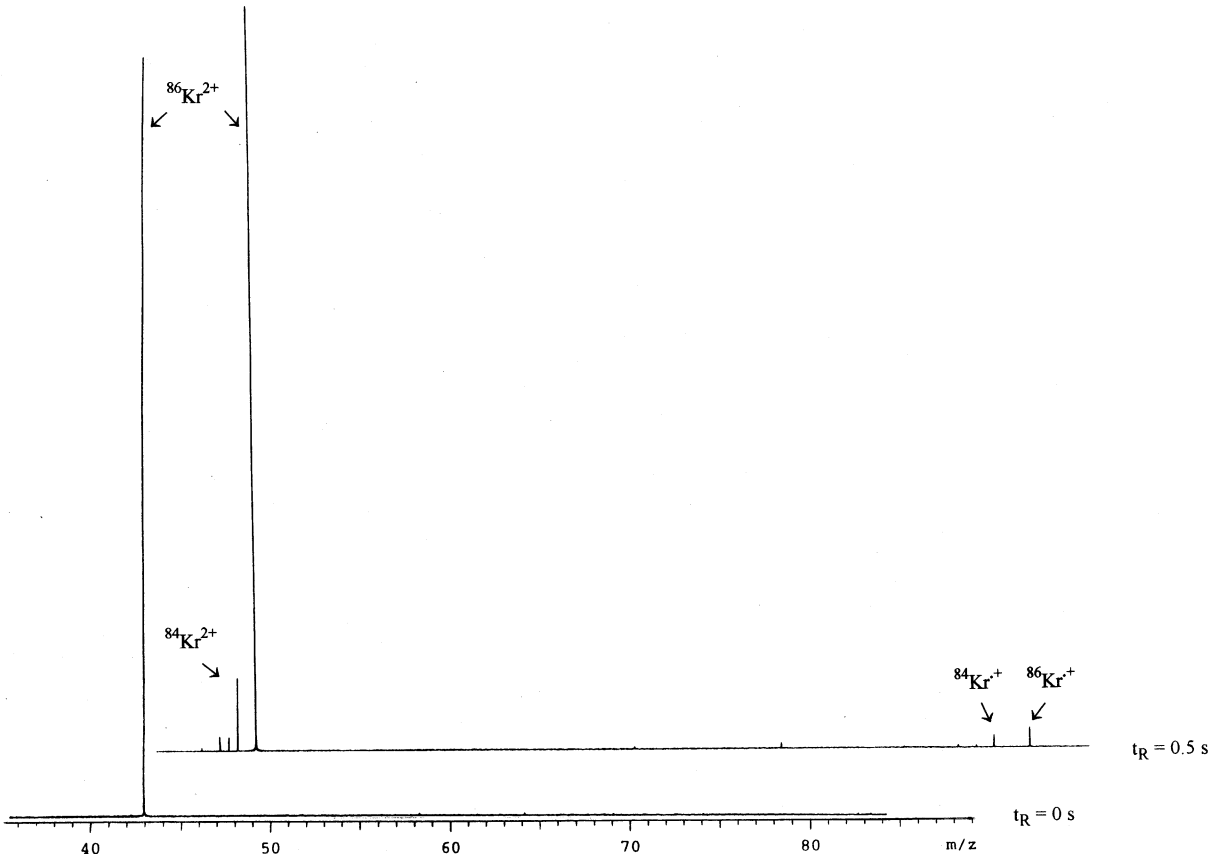

Fig. 4. Spectra showing the selection of $^{86}Kr^{2+}$ ions after ejection of all other ions from the FTICR cell at a neutral krypton gas pressure of 3.5×10^{-6} Pa (bottom) and the progress of the reaction of $^{86}Kr^{2+}$ ions with neutral krypton gas after a reaction time t_R of 0.5 s (top). Please note, that the induced image current of a single doubly charged ion is twice as high as compared with a single singly charged ion. Therefore, when the ratio between double electron transfer and single electron transfer is determined, the magnitude of the measured response signal corresponding to doubly charged ions has to be divided by a factor of two. The response signal was sampled for 26.2 ms and 400 digitized response signals were accumulated prior to Fourier transformation. For other conditions see Table 2.

beam, the remaining doubly charged ion intensity after interaction with the target gas, and the ion intensity because of the competing single electron transfer process. In this way the double electron transfer process turned out to be much more efficient than the single electron transfer process described by its cross section σ_{21}. The corresponding branching ratios σ_{20}/σ_{21} for the Ar^{2+}/Ar system range from 344–10.6 and for the Kr^{2+}/Kr system from 179–16.5 for the collision energy limits mentioned above.

These experimental observations can be discussed in the framework of electron capture processes by a doubly charged projectile colliding with an atom. These processes can be denoted by Scheme 1:

$$A^{2+} + {}^{o}A \rightarrow A^{+} + {}^{o}A + \Delta E \quad \text{(SEC)}$$
$$A^{2+} + {}^{o}A \rightarrow A + {}^{o}A^{2+} \quad \text{(DEC)}$$

where A is Ar, Kr or Xe, ^{o}A is the target atom in its isotopic abundance and ΔE the energy defect of the reaction. The recombination energies resulting from single electron capture processes are insufficient to open the pathway known as autoionization (compare second and fifth row in Table 3).

To our knowledge, all calculations performed on the systems we have studied experimentally take the entrance channel (A^{2+} + ^{o}A) into account which is dominated by the weak attractive polarization poten-

Table 3
Single and double charge transfer rate coefficients for the Xe^{n+}/Xe, Kr^{n+}/Kr and the Ar^{n+}/Ar systems, where $n = 1, 2$

Noble gas ion	Xe^{2+}	Kr^{2+}	Ar^{2+}
$E_{recombination}$ [eV]	^3P [21.2]	^3P [24.56]	^3P [27.62]
Lifetime	$^1S_0$ ($\tau \leq 15$ ms)[a]	$^1S_0$ ($\tau \leq 17.3$ ms)[a]	$^1S_0$ ($\tau \leq 159.7$ ms)[b]
Target gas	Xe	Kr	Ar
Ionization energy [eV]	^2P [12.13]	^2P [14.00]	^2P [15.76]
Reactant ion	$^{136}Xe^{\cdot+}$	$^{86}Kr^{\cdot+}$	$^{36}Ar^{\cdot+}$
Rate coefficient [$cm^3\ s^{-1}$]	2.9×10^{-10}	3.0×10^{-10}	3.4×10^{-10}
Reactant ion[c]	$Xe^{\cdot+}$	$Kr^{\cdot+}$	$Ar^{\cdot+}$
Rate coefficient [$cm^3\ s^{-1}$][c]	3.6×10^{-10}	3.4×10^{-10}	4.6×10^{-10}
Reactant ion	$^{136}Xe^{2+}$	$^{86}Kr^{2+}$	$^{40}Ar^{2+}$
Rate coefficient [$cm^3\ s^{-1}$]			
overall	3.4×10^{-10}	4.8×10^{-10}	5.4×10^{-10}
SEC[d]	1.6×10^{-10}	1.2×10^{-10}	1.4×10^{-10}
DEC[d]	1.8×10^{-10}	3.5×10^{-10}	3.9×10^{-10}

[a][40].
[b][41].
[c][42].
[d]SEC is single electron transfer and DEC is double electron transfer.

tial ($\propto$-$\alpha q^2/2R^4$, where α is the polarizability of ^oA and R is the internuclear distance) while the exit channel ($A^+ + {}^oA^+$) is dominated by the strong Coulomb repulsion ($\propto (q\text{-}1)/R$) [46]. These potential energy diagrams reveal no curve crossing at internuclear distances R which are in agreement with energy balance considerations. By using these prerequisites the agreement with experimental observations becomes worse if more than a single electron is allowed to participate in the charge transfer reaction so that electron correlation terms should be taken into account in the calculation of these potential energy diagrams. Another important parameter in the charge transfer process is the collision energy. The Langevin theory takes this parameter into account and predicts that the cross section σ inversely scales with the collision velocity. However, in symmetric charge transfer systems the prediction of correct transition probabilities fails because it does not fully describe the collision physics at near thermal energies [47]. Therefore quantum-mechanical models describing the collision physics of multi-electron systems are needed which account for the great variety of possible collision processes and the transitions which the active electrons can make both simultaneously or consecutively in a correlated fashion during a single collision. Unfortunately, to our knowledge there is at present no theory available to support or confirm by calculations the rate coefficients measured in this study for near thermal reactive ion/atom collisions.

4. Conclusions

The main objective of the present work has been to study symmetric single and double charge transfer processes by means of the FTICR mass spectrometric method in the near thermal collision energy range ($E_{coll} < 1$ eV) for singly and doubly charged rare gas ions in their parent gases. In the reaction of singly charged ions the determined rate coefficients show a good agreement with those provided by other methods. The rate coefficients in these reactions of $Ar^{\cdot+}$/Ar, $Kr^{\cdot+}$/Kr, $Xe^{\cdot+}$/Xe do not differ much from each other. In the reaction of doubly charged ions in their parent gases the overall rate coefficients increase from Xe^{2+}/Xe to Ar^{2+}/Ar. Even more remarkable is the as highly efficient observed process of double charge transfer from the reactant ion to the target atom within a single collision which contributes significantly more to the overall rate coefficient than the single charge transfer.

References

[1] W.G. Hormis, E.Y. Kamber, J.B. Hasted, A.G. Brenton, J.H. Beynon, Int. J. Mass Spectrom. Ion Processes 76 (1987) 263.
[2] E.Y. Kamber, W.G. Hormis, J.B. Hasted, A.G. Brenton, J.H. Beynon, J. Phys. B: At. Mol. Opt. Phys. 21 (1988) 3423.
[3] T. Kusakabe, T. Horiuchi, N. Nagai, H. Hanaki, I. Konomi, M. Sakisaka, J. Phys. B: At. Mol. Phys. 19 (1986) 2165.
[4] H. Andersson, G. Astner, H. Cederquist, J. Phys. B: At. Mol. Opt. Phys. 21 (1988) L187, and references cited therein.
[5] P. Hvelplund, A. Bárány, H. Cederquist, J.O.K. Pedersen, J. Phys. B: At. Mol. Opt. Phys. 20 (1987) 2515.
[6] R.H. Neynaber, S.Y. Tang, Chem. Phys. Lett. 92 (1982) 556.
[7] R. Johnsen, M.A. Biondi, Phys. Rev. A 20 (1979) 87.
[8] K. Okuno, T. Koizumi, Y. Kaneko, Phys. Rev. Lett. 40 (1978) 1708.
[9] F. Howorka, J. Chem. Phys. 67 (1977) 2919.
[10] D. Smith, D. Grief, N.G. Adams, Int. J. Mass Spectrom. Ion Phys. 30 (1979) 271.
[11] K.G. Spears, G.C. Fehsenfeld, M. McFarland, E.E. Ferguson, J. Chem. Phys. 56 (1972) 2562.
[12] W. Lindinger, E. Alge, H. Störi, M. Pahl, R.N. Varney, J. Chem. Phys. 67 (1977) 3495.
[13] H. Störi, E. Alge, H. Villinger, F. Egger, W. Lindinger, Int. J. Mass Spectrom. Ion Phys. 30 (1979) 263.
[14] R.E. Tosh, R. Johnsen, Int. J. Mass Spectrom. Ion Processes 123 (1993) 193.
[15] J.R. Gord, B.S. Freiser, S.W. Buckner, J. Chem. Phys. 94 (1991) 4282.
[16] T. Koizumi, K. Okuno, Y. Kaneko, J. Phys. Soc. Jpn. 53 (1984) 567.
[17] D. Smith, N.G. Adams, E. Alge, H. Villinger, W. Lindinger, J. Phys. B: At. Mol. Phys. 13 (1980) 2787.
[18] K. Soejima, K. Okuno, Y. Kaneko, Org. Mass Spectrom. 28 (1993) 344.
[19] H. von Köding, F.A. Pinkse, N.M.M. Nibbering, Rapid Commun. Mass Spectrom. 7 (1993) 780.
[20] H. von Köding, F.A. Pinkse, N.M.M. Nibbering, Phys. Scr. T59 (1995) 418.
[21] P. Caravatti, M. Allemann, Org. Mass Spectrom. 26 (1991) 514.
[22] XMASS software package is a trademark of Bruker Analytical Systems Inc. and Spectrospin AG.
[23] UNIX is a trademark of AT&T, New York, NY, USA.
[24] A.J.R. Heck, L.J. de Koning, F.A. Pinkse, N.M.M. Nibbering, Rapid Commun. Mass Spectrom. 5 (1991) 406.
[25] A.J.R. Heck, T. Drewello, L.J. de Koning, N.M.M. Nibbering, Int. J. Mass Spectrom. Ion Processes 100 (1990) 611.
[26] P. Kofel, M. Allemann, HP. Kellerhals, K.P. Wanczek, Int. J. Mass Spectrom. Ion Processes 74 (1986) 1.
[27] S.K. Huang, D.L. Rempel, M.L. Gross, Int. J. Mass Spectrom. Ion Processes 72 (1986) 15.
[28] D.L. Rempel, S.K. Huang, M.L. Gross, Int. J. Mass Spectrom. Ion Processes 70 (1986) 163.
[29] W.J. van der Hart, W.J. Guchte, Int. J. Mass Spectrom. Ion Processes 82 (1988) 17.
[30] W.J. Guchte, W.J. van der Hart, Int. J. Mass Spectrom. Ion Processes 95 (1990) 317.
[31] B.A. Hearn, C.H. Watson, G. Baykut, J.R. Eyler, Int. J. Mass Spectrom. Ion Processes 95 (1990) 299.
[32] Y. Naito, M. Inoue, Rapid Commun. Mass Spectrom. 11 (1997) 578.
[33] G.T. Uechi, R.C. Dunbar, J. Am. Soc. Mass Spectrom. 3 (1992) 734.
[34] T.J. Francl, M.G. Sherman, R.L. Hunter, M.J. Locke, W.D. Bowers, R.T. McIver Jr., Int. J. Mass Spectrom. Ion Processes 54 (1983) 189.
[35] T.-C.L. Wang, A.G. Marshall, Int. J. Mass Spectrom. Ion Processes 68 (1986) 287.
[36] L.J. de Koning, C.W.F. Kort, F.A. Pinkse, N.M.M. Nibbering, Int. J. Mass Spectrom. Ion Processes 95 (1989) 71.
[37] M.S. Kim, Int. J. Mass Spectrom. Ion Phys. 50 (1983) 189.
[38] C.E.C.A. Hop, T.B. McMahon, J. Phys. Chem. 95 (1991) 10582.
[39] R. Johnsen, M.A. Biondi Phys. Rev. A 18 (1978) 996.
[40] R.A. Walch, R.D. Knight, Phys. Rev. A 38 (1988) 2375.
[41] L. Yang, D.A. Church, S. Tu, J. Jin, Phys. Rev. A 50 (1994) 177.
[42] J.D.C. Jones, D.G. Lister, K. Birkinshaw, N.D. Twiddy, J. Phys. B: At. Mol. Phys. 13 (1980) 799.
[43] M.H. Prior, Phys. Rev. A 30 (1984) 3051.
[44] K.H. Kingdon, Phys. Rev. 21 (1923) 408.
[45] K. Okuno, J. Phys. Soc. Jpn. 55 (1986) 1504.
[46] Y. Kaneko, T. Iwai, S. Ohtani, K. Okuno, N. Kobayashi, S. Tsurubuchi, M. Kimura, H. Tawara, J. Phys. B: At. Mol. Phys. 14 (1981) 881.
[47] M. Pieksma, M. Gargaud, R. McCarroll, C.C. Havener, Phys. Rev. A 54 (1996) R13.